

*Journal of Organometallic Chemistry*, 240 (1982) 191–197  
 Elsevier Sequoia S.A., Lausanne – Printed in The Netherlands

## ELECTRONIC STRUCTURE OF $(\mu_2\text{-CO})[(\eta^5\text{-C}_5\text{H}_5)\text{Rh}(\text{CO})]_2$ BY UV PHOTOELECTRON SPECTROSCOPY AND CNDO CALCULATIONS

GAETANO GRANOZZI \*, EUGENIO TONDELLO,

*Istituto di Chimica Generale ed Inorganica, University of Padova, Via Loredan 4, 35100 Padova (Italy)*

DAVID AJÒ

*Istituto di Chimica e Tecnologia dei Radioelementi del C.N.R., Padova (Italy)*

and FELICE FARAONE

*Istituto di Chimica Generale, University of Messina, Messina (Italy)*

(Received June 7th, 1982)

### Summary

The electronic structure of  $(\mu_2\text{-CO})[(\eta^5\text{-C}_5\text{H}_5)\text{Rh}(\text{CO})]_2$  is discussed on the basis of the gas-phase UV photoelectron spectrum and CNDO quantum-mechanical calculations. The two lower ionization energy bands are assigned to ionizations from two MOs representing  $\text{Rh} \begin{array}{c} \text{CO} \\ \diagup \quad \diagdown \end{array} \text{Rh}$  and  $\text{Rh-Rh}$  bonding interactions, respectively. The results are compared with those previously reported for the  $\text{M} \begin{array}{c} \text{CH}_2 \\ \diagup \quad \diagdown \end{array} \text{M}$  triangular entity in analogous molecules. Evidence for a higher  $\pi$ -acceptor capability of  $\mu_2\text{-CH}_2$  compared with  $\mu_2\text{-CO}$  is reported.

### Introduction

The electronic structures of polynuclear organometallic molecules have been the object of several investigations involving theoretical and spectroscopical approaches [1]. The ultimate aim of these studies is the understanding of the nature of the multi-centered metal–ligand interactions which are thought to be similar in these cluster compounds to those in surface complexes formed on catalytic metal surfaces [2].

In the case of ligand-bridged diamagnetic polynuclear species, an important goal is to decide whether a direct metal–metal interaction or an indirect electron pairing via the bridging ligands is active. Recently, theoretical [3,4] and experimental (X–N maps [5], UV-PES [6,7]) data have shown that the picture of a direct metal–metal bond is inadequate in describing the electronic structures of  $(\mu_2\text{-CO})_3[\text{Fe}(\text{CO})_3]_2$ ,

$(\mu_2\text{-CO})_2[\text{Co}(\text{CO})_3]_2$ ,  $(\mu_2\text{-CO})_2[(\eta^5\text{-C}_5\text{H}_5)\text{Fe}(\text{CO})]_2$  and  $(\mu_2\text{-CO})_2[(\eta^5\text{-C}_5\text{H}_5)\text{Ni}]_2$ , all molecules containing two or more bridging carbonyls. These investigations favoured an indirect bonding via delocalized multicentered back-bonding interactions with bridging carbonyl  $\pi^*$  MOs.

This picture is formally very similar to that proposed [8] for the description of the electronic structure of  $(\mu_2\text{-CH}_2)[(\eta^5\text{-C}_5\text{H}_5)\text{Mn}(\text{CO})_2]_2$ , where the in-plane  $p_\pi$  empty methylene MO acts as an electron acceptor of metallic electrons via a back-bonding interaction. In this case, however, in contrast to the carbonyl bridged molecules mentioned above, a direct Mn–Mn interaction has also been indicated [8].

In extension of our previous investigations [6–8], we report here the gas-phase UV photoelectron (PE) spectrum of  $(\mu_2\text{-CO})[(\eta^5\text{-C}_5\text{H}_5)\text{Rh}(\text{CO})]_2$  (see Fig. 1).

The data obtained enabled us to make a comparison between the acceptor properties of  $\mu_2\text{-CO}$  and  $\mu_2\text{-CH}_2$ .

CNDO type calculations, which have been shown to be very accurate in describing the electronic structure of similar systems [6,8,9], have also been carried out for the title molecule in order to illuminate the bonding scheme and to provide a tool for the PE assignments.

## Experimental

The title compound was prepared by a slight modification [10b] of Lewis's method [10a].

He(I) and He(II) excited PE spectra were recorded on a Perkin–Elmer PS-18 spectrometer modified for He(II) measurements by inclusion of a hollow cathode discharge lamp which gives a high photon flux at He(II) wavelengths (Helectros Develop.) The spectrum was measured in the 70–85°C temperature range and was calibrated by reference to peaks due to added inert gases and to He  $1s^{-1}$  self-ionization.

Quantum mechanical calculations were performed by a version [11] of the CNDO method suitable for compounds containing transition metals. The geometrical data

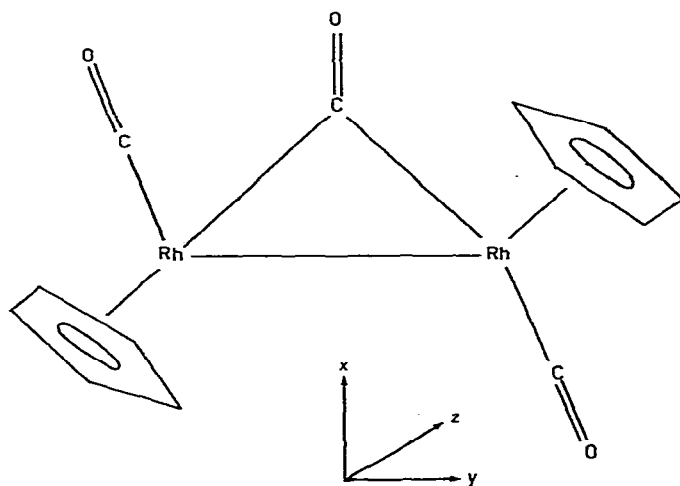


Fig. 1. Schematic view of the title molecule with the reference axes.

used in the calculations refer to the X-ray determination [12] ( $C_2$  point group). The computed eigenvalues were related to the measured ionization energies (IEs) through Koopmans' theorem [13]. Gross atomic charges and overlap populations were obtained by Mulliken's approach [14] applied to the deorthogonalized [15] CNDO eigenvectors.

## Results and discussion

The entire He(I) excited  $^3E$  spectrum of title molecule is shown in Fig. 2 together with the pertinent IEs (bands are labelled alphabetically). The lower IE spectral region (up to 11.5 eV) is the most interesting for discussing the bonding scheme since it includes ionizations from the valence MOs mainly involved into the interactions of

the  $\text{Rh} \begin{array}{c} \diagup \text{CO} \\ \diagdown \end{array} \text{Rh}$  triangle. Outer  $\pi$  cyclopentadienylic ionizations (those related to  $e_1'$  MO of the  $C_5H_5^-$  in  $D_{5h}$  symmetry) are also expected in this spectral region.

The higher IE region contains inner  $\pi$ - and  $\sigma$ -MOs of the  $C_5H_5$  rings and the  $5\sigma$ -,  $4\sigma$ - and  $1\pi$ -MOs peculiar to the carbonyl groups. However, the general appearance of this region, presenting broad and unresolved envelopes (H, I, J), prevents extraction of any useful informations.

At least eight different IE values can be picked out in the lower IE region; before attempting to rationalize this very complicated spectral pattern, some preliminary consideration is necessary.

The compound under study obeys the EAN rule; assuming the two Rh atoms in the formal oxidation state +1, we have 16 electrons in the whole molecule occupying  $4d$  metal based MOs. On the basis of qualitative considerations we expect that twelve of them will fill six MOs maintaining atom-like character (i.e. non-bonding)

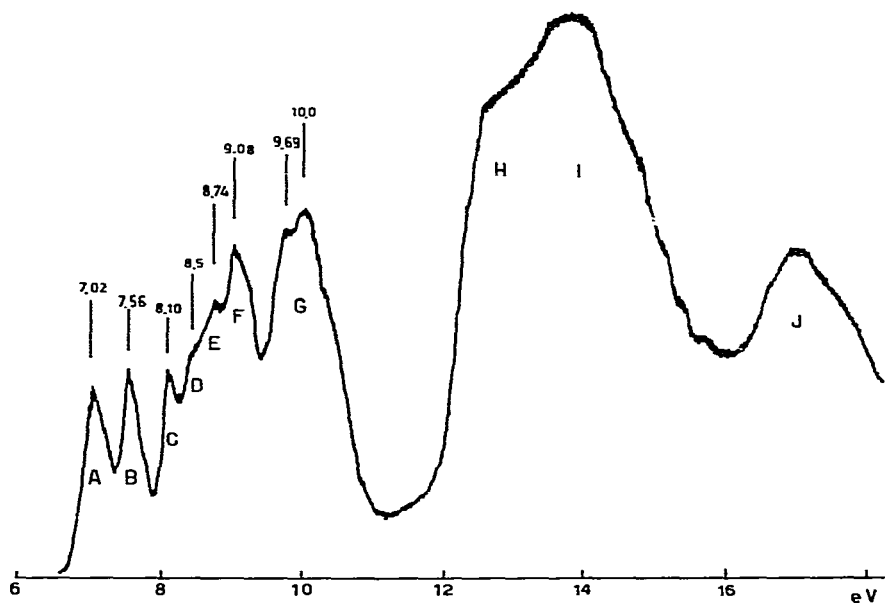


Fig. 2. He(I) excited PE spectrum of the title molecule.

whereas the remaining four electrons will be involved in the bonding of the  $(\mu_2\text{-CO})\text{Rh}_2$  core. The qualitative orbital interaction diagram shown in Fig. 3 summarizes this view; it was built up by interacting the valence basis sets of the two fragments CO and  $[(\eta^5\text{-C}_5\text{H}_5)\text{Rh}(\text{CO})]_2$  within the Extended Hückel scheme. The electronic structure of the latter fragment has been already discussed by Hofmann [16] in details: he predicted a Rh–Rh double bond with  $\pi$  character in the  $xy$  plane (see Fig. 1 for the axes choice). Only the frontier MOs which are relevant for interacting with the bridging CO are considered in Fig. 3: the Rh  $4d$  non-bonding MO and the Rh–C<sub>5</sub>H<sub>5</sub> bonding MOs are not individually represented in the diagram.

The interaction with the bridging carbonyl frontier orbitals ( $5\sigma$  and  $2\pi_{\perp, \parallel}^*$ ) mainly perturbs the  $\pi_{xy}^*$  and  $\sigma$  levels of the bimetallic fragment (Fig. 3): the Rh–Rh  $\sigma$  bond is strongly destabilized by the  $5\sigma$  carbonyl MO which points directly toward the Rh–Rh  $\sigma$ -bonding area whereas the  $\pi_{xy}^*$  and  $2\pi_{\parallel}^*$  fragment MOs mix significantly

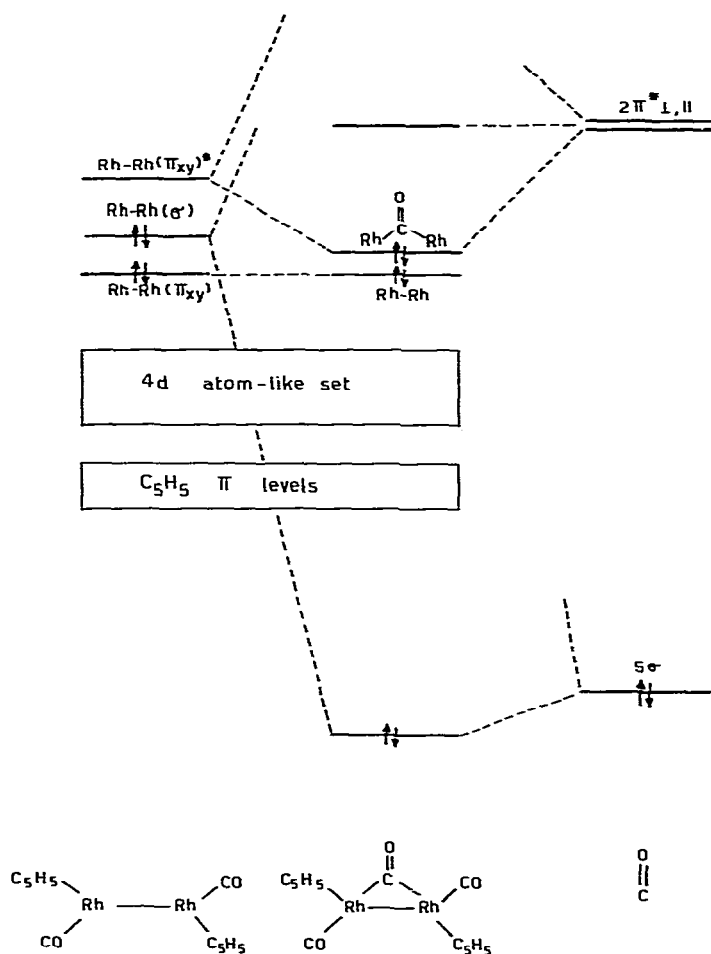


Fig. 3. Orbital interaction diagram of the title molecule from its constitutive  $[(\eta^5\text{-C}_5\text{H}_5)\text{Rh}(\text{CO})]_2$  and  $\mu_2\text{-CO}$  fragments.

giving rise to a  $\text{Rh} \begin{array}{c} \diagup \text{CO} \\ \diagdown \end{array} \text{Rh}$  bonding MO. This qualitative picture predicts, then, for the whole molecule two high-lying very close in energy occupied MOs representing Rh–Rh and  $\text{Rh} \begin{array}{c} \diagup \text{CO} \\ \diagdown \end{array} \text{Rh}$  bonding interactions. Significant bending from the internuclear axes is predicted for these bonds, and the similarity of these two MOs with the  $e'$  Walsh-like MO of cyclopropane [17],  $M_3$  [9,18] and  $M_2\text{CH}_2$  [8] triangles is to be stressed. Similarly, the low-lying  $5\sigma$ -carbonyl MO is to be related to the  $a_1$  Walsh-type MO [8,9,17,18]. It is also of interest to note the Rh–Rh antibonding character residing in the  $\text{Rh} \begin{array}{c} \diagup \text{CO} \\ \diagdown \end{array} \text{Rh}$  MO.

These qualitative considerations find a direct counterpart in the CNDO results reported in Table 1. As found in other cases [8,9], this semiempirical method can provide useful indications, especially for those molecular systems whose complexity prevents the use of more accurate quantum-mechanical tools. It should be emphasized, however, that the correct approach with such semiempirical methods requires both a systematic check against the experimental data and common sense. In fact, the data in Table 1 compare satisfactory with the experimental IEs of Fig. 2 (connected via the Koopmans' theorem), especially when the relative energy ordering is considered; in particular, the  $4d$  atom-like ionizations (from  $24a$  to  $21b$  MOs of Table 1) span over 1 eV, in agreement with the experimental range relative to bands C, D, E, and F. Moreover, with respect to the  $4d$  MOs, two MOs ( $24b$  and  $25a$ ) are predicted at lower IEs and a group of four  $\pi\text{-C}_5\text{H}_5$  MOs ( $20b$ ,  $21a$ ,  $19b$ ,  $20a$ ) at higher IEs. These results, together with the comparison of the spectrum of Fig. 2 with previous results of related cyclopentadienyl complexes [19], lead us to put forward with reasonable confidence the following assignments: bands C, D, E, and F we take to represent  $4d$  ionizations, whereas band G is related to four  $\pi\text{-C}_5\text{H}_5$  MOs. He(II) intensity measurements strongly support these assignments, since they show a marked intensity growth for bands C, D, E, and F associated to the  $4d$  lone

TABLE 1

CNDO EIGENVALUES AND EIGENVECTORS FOR  $(\mu_2\text{-CO})[(\eta^5\text{-C}_5\text{H}_5)\text{Rh}(\text{CO})]_2$ 

MO	Eigen value (eV)	Population (%)					Dominant character
		Rh(5sp)	Rh(4d)	$\mu_2\text{-CO}$	CO	$\text{C}_5\text{H}_5$	
$24b$ (HOMO)	-8.75	10	50	10	4	26	Rh–CO–Rh bonding
$25a$	-9.15	17	50	0	5	28	Rh–Rh bonding
$24a$	-10.36	1	92	0	3	4	} $4d$ "atom-like" MOs (non-bonding)
$23b$	-10.72	2	86	7	0	5	
$23a$	-10.83	2	90	0	2	6	
$22b$	-10.92	0	91	1	3	5	
$22a$	-10.96	2	93	2	2	2	
$21b$	-11.30	0	89	3	5	4	
$20b$	-11.94	4	19	3	0	74	} $\pi\text{-C}_5\text{H}_5$ MOs with some metal contribution
$21a$	-11.95	3	21	0	1	75	
$19b$	-12.68	3	33	1	0	63	
$20a$	-12.69	4	32	0	0	64	

pairs. The only reasonable doubt lies in the relative assignment of bands A and B to the 24*b* and 25*a* MOs. Based on the CNDO results, we tentatively relate the band A to the HOMO 24*b* representing the Rh— $\overset{\text{CO}}{\text{---}}$ —Rh multicentered back-bonding

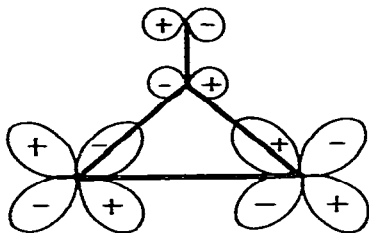


Fig. 4. Rh— $\overset{\text{CO}}{\text{---}}$ —Rh multicentered back-bonding interaction.

interaction as shown in Fig. 4 and the band B to the Rh—Rh direct bonding. However, this assignment requires further evidences to be considered definitive.

The comparison of these results with those reported previously [8] for the molecule containing the Mn— $\overset{\text{CH}_2}{\text{---}}$ —Mn ring enables us to discuss the relative  $\pi$  acceptor capabilities of  $\text{CH}_2$  and CO; in the manganese case the ionization from the Mn— $\overset{\text{CH}_2}{\text{---}}$ —Mn bonding MO lies 1.70 eV higher than that from the Mn—Mn bonding MO. This is a clear indication of a higher  $\pi$ -acceptor capability of  $\text{CH}_2$ , even if the comparison is weakened by the difference in the donor properties between  $\text{Mn}^{\text{I}}$  and  $\text{Rh}^{\text{I}}$  atoms. A better comparison would involve data for  $(\mu_2\text{-CH}_2)[(\eta^5\text{-C}_5\text{H}_5)\text{Rh}(\text{CO})]_2$ .

The computed gross atomic charges and overlap populations reported in Table 2 permit further observations to be made. The high electron density of the two Rh atoms, which are very near to neutrality in contrast with the formal oxidation state, and the small positive charge carried by the bridging carbonyl are noteworthy. These results, when compared with those reported for the methylene-bridged manganese molecule [8], are consistent with the already mentioned lower  $\pi$ -acceptor property of CO with respect to  $\text{CH}_2$ . The overlap population between Rh and bridging CO indicates a strong bond, comparable with the Rh—CO terminal one. A final remark

TABLE 2

GROSS ATOMIC CHARGES AND RELEVANT OVERLAP POPULATIONS FOR  $(\mu_2\text{-CO})[(\eta^5\text{-C}_5\text{H}_5)\text{Rh}(\text{CO})]_2$ <sup>a,b</sup>

Rh	+0.02	Rh—Rh	0.098
C'	+0.44	Rh—C'	0.440
O'	-0.38	Rh—C''	0.350
C''	+0.57	C'—O'	1.030
O''	-0.45	C''—O''	1.001
C <sub>5</sub> H <sub>5</sub>	-0.14	Rh—C <sub>5</sub> H <sub>5</sub>	0.660

<sup>a</sup> Average values (in  $e^-$ ). <sup>b</sup> C', O' refer to terminal carbonyls and C'', O'' to  $\mu_2$ -CO.

concerns the Rh–Rh total overlap population: the actual value ( $0.098 e^-$ ) is small compared to corresponding values of other metal–metal bonds involving second series transition metals ( $0.2\text{--}0.3 e^-$ ). This probably reflects the Rh–Rh antibonding character which is located in the  $24b$  HOMO.

## Conclusions

The proposed picture of the electronic structure of the title compound, particularly as regards the three-membered ring, indicates that the Rh–Rh and Rh– $\begin{array}{c} \text{CO} \\ \diagup \quad \diagdown \end{array}$ –Rh bonds are the highest occupied MOs, and that they are close in energy; this represents the major difference with respect to the M– $\begin{array}{c} \text{CH}_2 \\ \diagup \quad \diagdown \end{array}$ –M ring where the M–M HOMO lies at significantly lower IEs with respect to the M– $\begin{array}{c} \text{CH}_2 \\ \diagup \quad \diagdown \end{array}$ –M MO. These results can be interpreted in terms of the better  $\pi$ -acceptor property of  $\mu_2$ -CH<sub>2</sub> compared with  $\mu_2$ -CO.

## Acknowledgement

This work was supported in part by the Italian Consiglio Nazionale delle Ricerche (C.N.R.) (CT80.02550.03).

## References

- 1 M.C. Manning and W.C. Trogler, *Coord. Chem. Rev.*, 38 (1981) 89 and refs. therein.
- 2 E.L. Muettterties, T.N. Rhodin, E. Band, C.F. Bruker and W.R. Pretzer, *Chem. Rev.*, 79 (1979) 91.
- 3 (a) M. Bènard, *J. Amer. Chem. Soc.*, 100 (1978) 7740; (b) M. Bènard, *Inorg. Chem.*, 18 (1979) 2782.
- 4 W. Heijser, E.J. Baerends and P. Ros, 14th Faraday Symposium, (1980) 211.
- 5 A. Mitscher, B. Rees and M.S. Lehmann, *J. Amer. Chem. Soc.*, 100 (1978) 3390.
- 6 G. Granozzi, E. Tondello, M. Bènard and I. Fragalà, *J. Organometal. Chem.*, 194 (1980) 83.
- 7 G. Granozzi, M. Casarin, D. Ajò and D. Osella, *J. Chem. Soc., Dalton Trans.*, in press.
- 8 G. Granozzi, E. Tondello, M. Casarin and D. Ajò, *Inorg. Chim. Acta*, 48 (1981) 73.
- 9 D. Ajò, G. Granozzi, E. Tondello and I. Fragalà, *Inorg. Chim. Acta*, 37 (1979) 191.
- 10 (a) J. Evans, B.F.G. Johnson, J. Lewis and J.R. Norton, *J. Chem. Soc., Chem. Commun.*, (1973) 79; (b) F. Faraone, S. Lo Schiavo, G. Bruno, P. Piraino and G. Bombieri, submitted for publication.
- 11 E. Tondello, *Inorg. Chim. Acta*, 11 (1974) L5.
- 12 O.S. Mills and J.P. Nice, *J. Organometal. Chem.*, 10 (1967) 337.
- 13 T.C. Koopmans, *Physica*, 1 (1934) 104.
- 14 A.S. Mulliken, *J. Chem. Phys.*, 23 (1955) 1833.
- 15 P.O. Löwdin, *J. Chem. Phys.*, 18 (1950) 365.
- 16 P. Hofmann, *Angew. Chem. Int. ed. Engl.*, 18 (1979) 554.
- 17 A.D. Walsh, *Trans Farad. Soc.*, 45 (1949) 179.
- 18 B.E.R. Schilling and R. Hoffmann, *J. Amer. Chem. Soc.*, 101 (1979) 3456.
- 19 J.C. Green, *Struct. Bonding (Berlin)*, 43 (1981) 37.